Engineered Science
DOI: https://dx.doi.org/10.30919/es1259

Evaluation of Autogenous Shrinkage and Thermal Behavior of Cellulose Fiber and Synthetic Fiber Reinforced High-strength Concrete

Panisa Sangkeaw,[1] Karen Midori Masunaga,[2] Takeshi Iyoda[3] and Chanachai Thongchom[1,*]

Abstract

High-strength concrete (HSC) can encounter challenges such as cracking during the hardening process, primarily attributed to early-age shrinkage. One strategy to mitigate shrinkage involves introducing various materials into the concrete mix. This study sought to evaluate the addition of cellulose fiber (CF), glass fiber (GF), and polypropylene fiber (PPF) on the autogenous shrinkage and thermal behavior of high-strength concrete. When comparing HSC with fiber and HSC without fiber, the results indicated that the addition of GF, particularly at a 1% proportion, could decrease shrinkage by 69.9%, yielding the most effective reduction in shrinkage. CF also exhibited shrinkage reduction benefits at a 1% fiber ratio, decreasing shrinkage by 39.7%, while PPF performed well with a 0.5% fiber addition, decreasing shrinkage by 24.4%. The thermal behavior of HSC showed a peak at approximately 160 °C across all three samples, and fibers could decrease the internal pore pressure, boosting their effectiveness as an additive to mitigate spalling at elevated temperatures.

Keywords: High strength concrete; Autogenous shrinkage; Cellulose fiber; Synthetic fiber; Concrete.
Received: 14 March 2024; Revised: 03 September 2024; Accepted: 06 September 2024.
Article type: Research article.

1. Introduction

High-strength concrete (HSC) stands as one of the most advanced building materials. It is particularly valued for its application in infrastructure projects requiring exceptional strength and long-term durability. An inherent challenge with HSC lies in the deformation caused by concrete autogenous shrinkage, which is a primary factor contributing to the formation of cracks.[1-3] To address this concern, various types of fibers, encompassing natural and synthetic varieties, have been integrated into HSC formulations.[4]

The research underscores the benefits of introducing cellulose fibers into concrete, aiding in the control of drying shrinkage and the mitigation of plastic cracking. However, research regarding their impact on autogenous contraction remains limited. Cellulose fibers exhibit excellent dispersion within hydrating cement paste, facilitating water absorption and release. This property makes them suitable candidates for use as internal curing materials. Previous studies have explored the influence of natural fibers, such as kenaf and cellulose fibers, on the autogenous shrinkage of cement paste. These fibers have been proven to be effective in reducing shrinkage and curtailing the formation of small cracks.[5,6] The effect of 0.25% kenaf fiber on the autogenous shrinkage of cement decreased the shrinkage of the material by 16.74%.[7] Investigations into the effects of jute, hemp, and abaca fibers on the autogenous shrinkage of mortar have demonstrated their capacity to significantly reduce autogenous shrinkage,[8] primarily due to the release of excess water by the fibers during the initial stages of hydration to compensate for moisture loss during the hydration reaction. Furthermore, these fibers bridge microcracks within the cement matrix,

[1] *Thammasat University Research Unit in Structural and Foundation Engineering, Department of Civil Engineering, Thammasat School of Engineering, Thammasat University, 99 Phahonyothin Road, Khlong Nueng, Khlong Luang City, Pathum Thani 12120, Thailand.*
[2] *Graduate School of Engineering and Science, Shibaura Institute of Technology, 3-7-5 Toyosu, Koto-ku City, Tokyo 1358548, Japan.*
[3] *Department of Civil Engineering, Shibaura Institute of Technology, 3-7-5 Toyosu, Koto-ku City, Tokyo 1358548, Japan.*
**Email:* Tchanach@engr.tu.ac.th (C. Thongchom)

effectively restraining crack propagation.[9]

Polypropylene strands are known for their ability to minimize deformation in cementitious composite materials, particularly in the context of autogenous contraction, plastic shrinkage, and restrained shrinkage. The inclusion of fibers contributes to a reduction in crack formation during the initial 12 hours of autogenous shrinkage of the concrete.[10] These fibers also enhance the mechanical properties of concrete, increasing its strength and stress-bearing capacity. Controlling small cracks holds paramount importance for ensuring long-term durability, as small cracks may eventually evolve into more extensive fissures.[11] Research has also delved into the impact of various fractions of polypropylene fibers, indicating that fiber contents of 0.25%, 0.5%, and 0.75% result in shrinkage reductions of 5%, 15%, and 26%, respectively, after 24 hours of concrete aging. Saturated fibers in concrete further reduce shrinkage, narrowing the crack width and positively affecting overall shrinkage.[12] Additionally, studies have explored the addition of polypropylene fibers to concrete as a means of controlling small cracks arising from autogenous shrinkage, free shrinkage, and restrained shrinkage. The findings reveal that recycled polymer fibers can serve as viable alternatives to polypropylene fibers, albeit requiring higher quantities. During the early stages of concrete hardening, research indicates the efficacy of steel fibers, plastic fibers, and glass fibers in reducing concrete shrinkage, with a fiber content of 0.38% being identified as effective.[13]

As the utilization of high-strength concrete continues to increase, so does the associated risk of exposure to high temperatures. The response of high-strength concrete to elevated temperatures differs markedly from that of conventional concrete. Consequently, investigating the behavior of high-strength concrete is of considerable interest, as the resultant test findings could be applied in cutting-edge industries requiring specialized concrete resilient to specific temperature conditions.[14] Past research has delved into the behavior of both normal and high-strength concrete when subjected to thermal cycles utilizing thermogravimetric analysis (TGA). The outcomes highlight that high-strength concrete, when heated to 400 °C, experiences more pronounced adverse effects than normal concrete.[15] HSC contains silica fumes to help increase its compressive strength. However, the presence of silica fumes in the mixture may pose a risk of spalling within the matrix. To reduce this problem, one method that may help reduce spalling is the selective addition of fibers to high-strength concrete mixtures.[16] There are also reports suggesting that fibers with a low melting point can mitigate the internal water vapor pressure within high-strength concrete, thus preventing the spalling of the concrete as a consequence of the formation of a porous network above the melting point of the fibers. Previous studies have assessed the thermal properties of HSC reinforced with steel fibers by TGA. When the initial temperature reaches 800 °C, the mass loss of HSC reinforced with steel fibers is similar to that of HSC without fibers. However, the mass loss of HSC reinforced with steel fibers decreases slightly when the temperature is higher than 800 °C.[17]

Given the current lack of research on the concept of autogenous shrinkage in fiber-reinforced high-strength concrete, this study aimed to evaluate the effects of cellulose fibers derived from pulp waste material, as well as two types of synthetic fibers-polypropylene and glass fibers-on autogenous shrinkage and thermal behavior. An overview of the research is shown in Fig. 1.

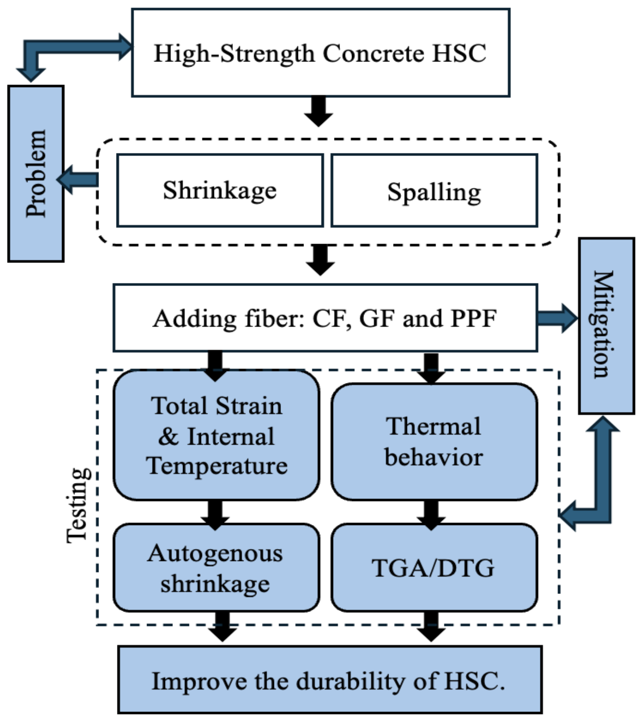

Fig. 1 Overview of the research.

2. Experimental program

2.1 Materials

In this study, Ordinary Portland Cement (OPC) was used as hydraulic cement according to the ASTM C1157 standard.[18] River sand served as the fine aggregate, while coarse aggregates consisted of limestone flakes with a maximum particle size of 9.5 mm. The incorporation of a water-reducing agent with sodium lignosulfonate as the primary component was in accordance with the ASTM C494 standard.[19] To enhance the compressive strength, silica fume was used in the form of microsilica according to ASTM C618.[20] Cellulose fiber (CF) boasts an 88% cellulose content and is derived from wastepaper pulp extracted from wood. In this study, CF was saturated in water for 24 hours prior to mixing. The cellulose fibers functioned as internal curing agents, playing a role in maintaining the moisture balance within the concrete. Polypropylene fiber (PPF) is comprised of highly flexible synthetic petroleum-based fibers that significantly contribute to improving crack performance, while glass fibers (GF) play a vital role in reinforcing and enhancing crack resistance, thereby countering tensile forces in concrete. Table 1 shows the physical properties of the fibers.

2.2 Mixture proportions

The proportions for high-strength concrete mixtures were selected according to ACI 211.[21] These mixtures were categorized into sample groups for testing, as indicated in Table 2. In each high-strength concrete sample, fibers 0.5% or 1% by weight of the cement were incorporated. The symbols in the table are defined as follows: FA = fine aggregate, CA = coarse aggregate, WR = water reducer, CF = cellulose fiber, PPF = polypropylene fiber, and GF = glass fiber. All the samples maintained a consistent water-to-binder (w/b) ratio of 0.26.

2.3 Test methods

For preparing the test sample, the autogenous shrinkage test involves several steps. The initial step involves preparing the

Table 1. Physical properties of the fibers.

Fiber	Picture	Length (mm.)	Diameter (mm.)	Density (kg/m^3)	Tensile strength (MPa)	Melting point (°C)
Cellulose Fiber: CF		2.1	0.018	1100	600-900	270-300
Glass Fiber: GF		6	0.013	2500	>800	900-1000
Polypropylene Fiber: PPF		6	0.02	910	500-700	160-170

Table 2. High-strength concrete mixture proportions.

Mixture	Sample groups						
	HSC Control	HSC CF0.5%	HSC CF1%	HSC GF0.5%	HSC GF1%	HSC PPF0.5%	HSC PPF1%
Cement kg/m^3	526	526	526	526	526	526	526
SF kg/m^3	28	28	28	28	28	28	28
FA kg/m^3	780	780	780	780	780	780	780
CA kg/m^3	1002	1002	1002	1002	1002	1002	1002
Water kg/m^3	142	142	142	142	142	142	142
WR kg/m^3	32	32	32	32	32	32	32
CF kg/m^3	-	2.6	5.3	-	-	-	-
GF kg/m^3	-	-	-	2.6	5.3	-	-
PPF kg/m^3	-	-	-	-	-	2.6	5.3

molds for concrete placement. The molds, measuring 150×150×450 mm, are covered with a Neoprene rubber sheet to prevent any concrete leakage. Inside the mold, there is an embedded gauge bolt plug. Following the mixing of the concrete, the second step entails pouring it into a prepared mold, followed by inserting a K-type thermocouple at the center of the concrete, and connecting the thermocouple wire to a thermometer. Temperature measurements were taken at 30-minute intervals. In the third step, the upper surface of the concrete is sealed using multiple layers of polyester film. This helps to prevent moisture evaporation. Additionally, any gaps or joints in the mold must be sealed with aluminum tape to reduce moisture exchange between the sample and the surrounding environment. The fourth step involves installing the sample for measuring autogenous shrinkage. This is achieved by using a linear variable differential transformer (LVDT), which is placed in contact with the gauge bolt plug embedded in the concrete sample. Subsequently, the LVDT is connected to both a data logger and a computer to facilitate shrinkage measurements. The shrinkage test was conducted within a controlled room. The temperature was maintained at a stable room temperature of 20 ± 2 °C and a relative humidity of 60 ± 5%.[22,23] The autogenous shrinkage measurement started at the final setting time of the sample. The strain values were recorded from hour 0 until 168 hours. The autogenous shrinkage test procedure is illustrated in Figs. 2 and 3. The autogenous shrinkage and thermal behavior were tested using the average results from three samples. Each sample was tested under identical conditions to ensure the reliability and reproducibility of the results.

When conducting thermal analysis, specifically thermogravimetric analysis (TGA) and differential thermal analysis (DTG), the following testing procedure was utilized: A fragment sample was tested for 7 days and subsequently cured in a climate room at 50% relative humidity. The sample holder comprised 70 µl of alumina and weighed approximately 500 milligrams. Once the concrete sample reached a consistent weight, it was transferred to an aluminum tray. The next step involved introducing the sample into the testing machine. Subsequently, the sample was heated progressively at a rate of 10 °C per minute until the temperature reached 1000 °C. All of this occurred under ambient conditions with a flow rate of 30 ml/min.[8]

Thermogravimetric analysis (TGA/DTG) was used to evaluate the effect of high-temperature conditions on the thermal mass stability of HSC. When HSC is exposed to high temperatures, it is more likely to experience spalling than conventional concrete due to its high density and decreased permeability. Elevated temperatures above 100 °C lead to the release and vaporization of water in the concrete (free, capillary, adsorbed, and chemically bound water), and the pore pressures combined with thermal stress from the temperature gradient and shrinkage cause internal stresses to appear. Exceeding the tensile strength, thermal cracks and spalling can occur because the use of fibers is recommended and adopted to prevent and mitigate thermal cracks and spalling. In this study, internal stress was not evaluated, and TGA/DTG was used instead, primarily to understand the interaction between high temperature and water evaporation behavior in HSC. Additionally, the decomposition of hydration products and the degradation of fibers were investigated.

3. Results and discussion

3.1 Fresh properties

Table 3 presents the findings from the HSC slump and air content tests, which offer insight into the performance of fresh concrete. Analysis of the slump results revealed that the control sample exhibited more slump than the samples containing CF and GF fibers, with 1% fiber showing a slump lower than 0.5%. However, PPF at 1% showed a higher slump at 0.5%. Furthermore, the air content results of HSC indicate that samples containing all three fiber types had lower air

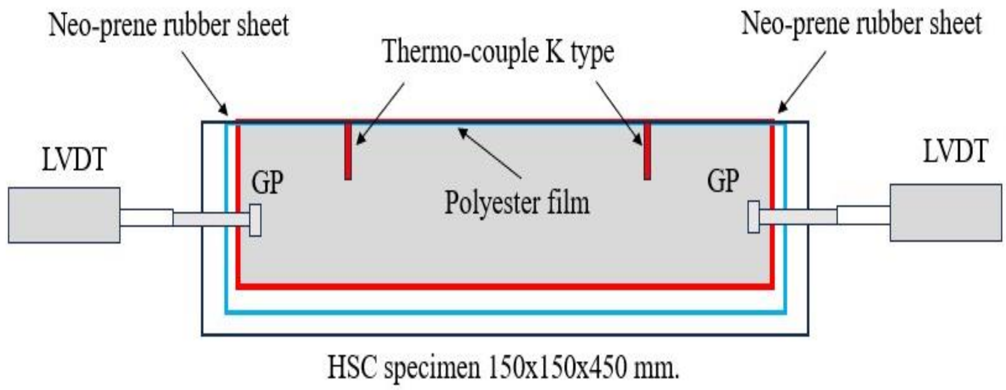

Fig. 2 Schematic diagram showing the measurement of autogenous shrinkage.

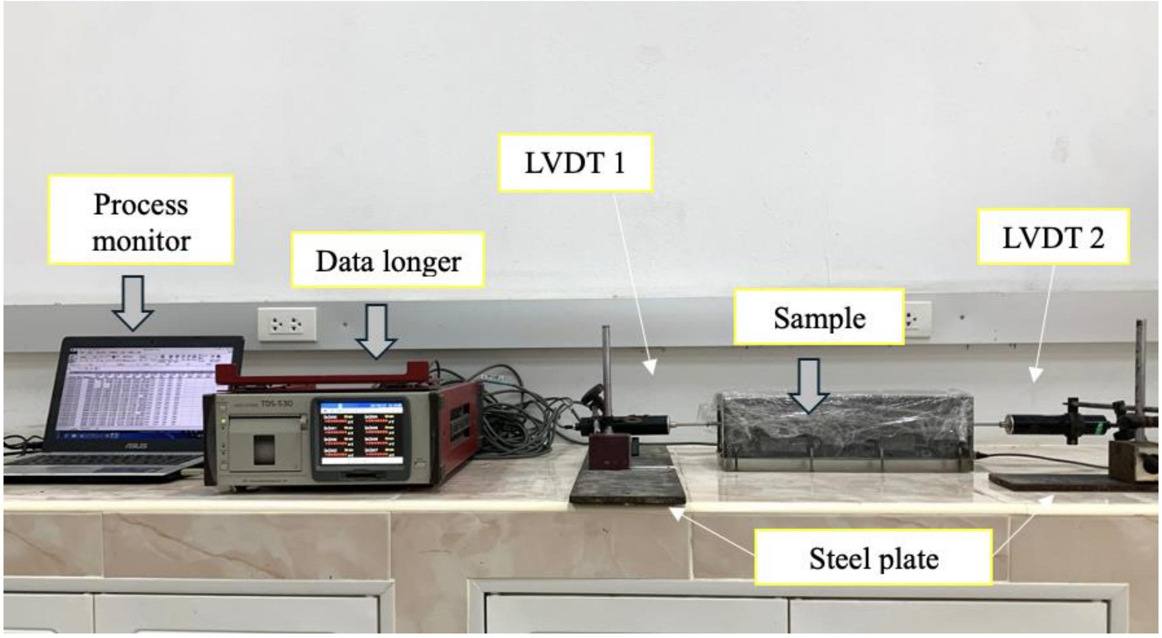

Fig. 3 Autogenous shrinkage test.

contents than the control sample. Notably, the samples with a CF and a GF of 1% displayed lower air content than those with a CF and a GF of 0.5%, while the PPF at 1% showed a higher air content at 0.5%. These findings indicate the significant effect of fibers on slump and air content. Functional efficacy can be attributed to the even distribution of fibers, which likely contributes to the satisfactory performance of fresh HSC.

Table 3. Slump and air content of HSC.

Mixture	Slump (mm.)	Air content (%)
HSC-Control	111	4.6
HSC-CF0.5%	91	3.8
HSC-CF1%	87	3.5
HSC-GF0.5%	76	3.2
HSC-GF1%	72	2.8
HSC-PPF0.5%	86	3.7
HSC-PPF1%	89	3.9

The results of the setting time tests are presented in Table 4. When evaluating the initial and final setting times of HSC supplemented with CF, GF, and PPF, it was observed that the initial and final setting times of the fiber-added samples were faster than those of the control sample. Furthermore, the initial and final setting times accelerated as the fiber proportion increased.

3.2 Internal temperature

Variations in temperature within the concrete can lead to thermal deformations, which, in turn, affect the hydration reaction of the cement matrix and the autogenous shrinkage of the concrete. Fig. 4 shows the correlation between internal temperature and age. According to the test results, all the samples exhibited similar internal temperature values. The temperature within the test samples exhibited significant fluctuations during the initial rapid cement hydration phase, peaking at approximately 12 hours after the concrete was mixed. Subsequently, the temperature gradually stabilized, converging toward a chamber temperature of 20 °C. This observation aligns with the findings of Shen *et al.* (2020),[2] who suggested that temperature changes are more influenced by the quality and quantity of cement and water than by the presence of fibers.

Table 4. Results of the setting times.

Mixture	Initial setting time (min)	Final setting time (min)
HSC-Control	310	513
HSC-CF0.5%	260	421
HSC-CF1%	225	393
HSC-GF0.5%	189	388
HSC-GF1%	153	362
HSC-PPF0.5%	266	428
HSC-PPF1%	252	392

3.3 Thermal expansion

The results from the thermal expansion test can be determined by multiplying the thermal expansion coefficient by the internal temperature difference of the sample, as illustrated in Fig. 5. Notably, all the samples exhibited peak expansion at approximately 13 to 14 hours. Specifically, HSC-Control peaked at a point expansion of 79 $\mu\varepsilon/°C$, whereas HSC-CF, HSC-GF, and HSC-PPF showed peak points of 82, 85, and 78 $\mu\varepsilon/°C$, respectively. Previous studies by Yoo *et al.* (2013)[3]

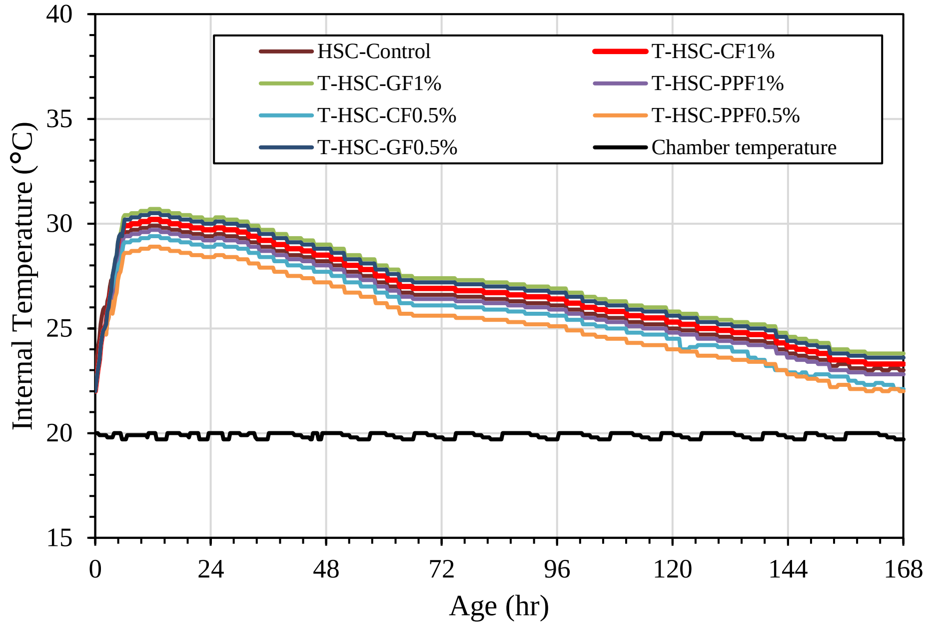

Fig. 4 Relationship between internal temperature and age.

suggested that thermal expansion compensates for autogenous shrinkage. However, the results of the thermal expansion test indicate that all samples exhibited similar thermal expansion values.

3.4 Total shrinkage

Figures 6-9 illustrate the correlation between total shrinkage and the age of the HSC-GF, HSC-CF, and HSC-PPF. The strain depicted in the graphs can be quantified through testing and constitutes the total shrinkage. All samples exhibited similar total contractions before 7 hours.

Figure 6 shows that the HSC-CF sample containing 1% cellulose fibers had lower shrinkage than that for the sample with 0.5% fiber content. Additionally, the inclusion of cellulose fibers resulted in reduced shrinkage compared to that of the control sample. This trend was evident in the HSC-Control, HSC-CF 0.5%, and HSC-CF 1% aged for 7 days, which displayed shrinkage values of 350 με, 242 με, and 218 με, respectively. The decreases in total shrinkage were 30.9% and 37.7%, respectively. The study findings align with prior research by Kurpinska *et al*. (2022),[24] which investigated the use of natural fibers to mitigate total shrinkage in cement composites. The research revealed that samples lacking fibers and those containing cotton fibers exhibited the highest total shrinkage rates. In contrast, sisal fiber samples showed minimal total shrinkage. These results suggest that fiber

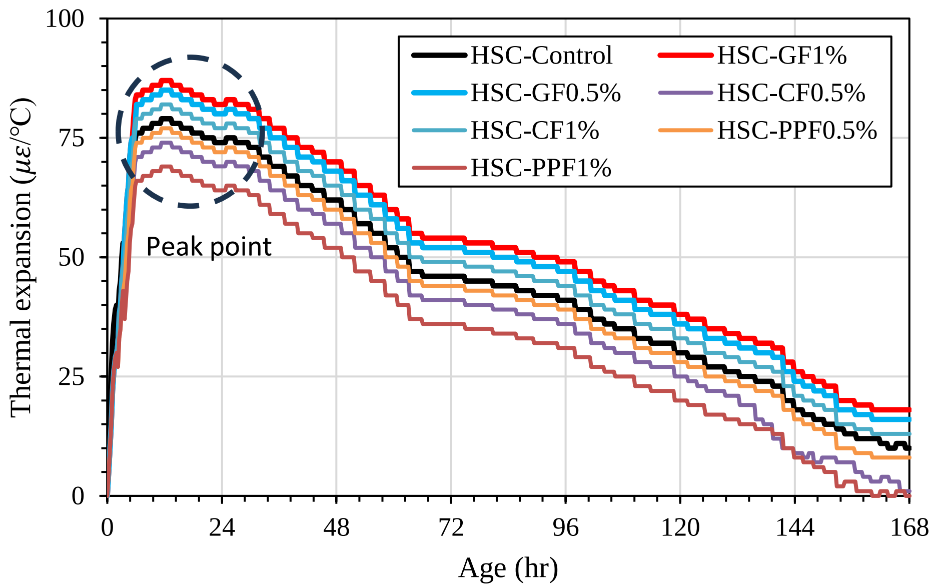

Fig. 5 Relationship between thermal expansion and age.

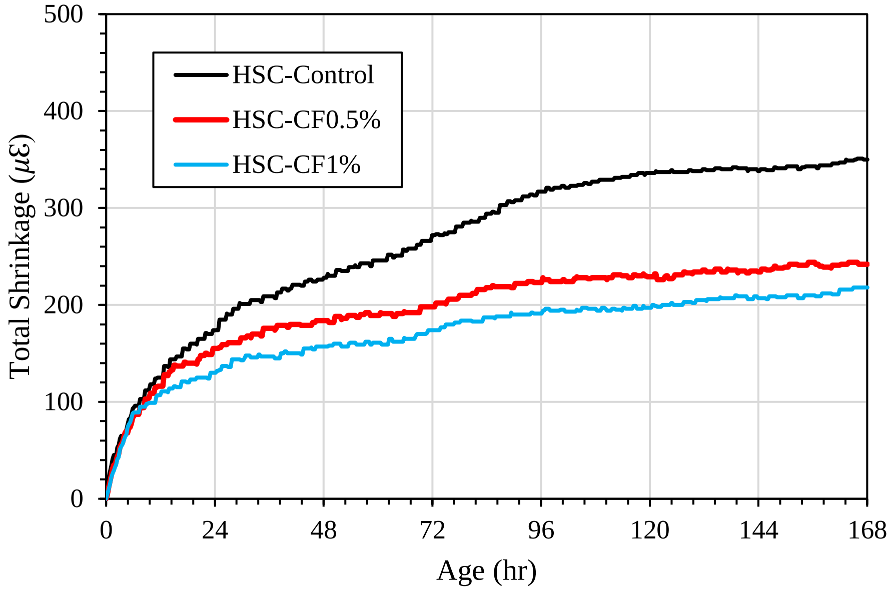

Fig. 6 Relationship between total shrinkage and age of HSC-control, HSC-CF0.5% and 1%.

characteristics such as structure, diameter, cellulose content, and total length within the composition have an influence on total shrinkage.

An analysis (Fig. 7) of the HSC-GF revealed that the total shrinkage of the sample with a 1% proportion of glass fibers was lower than that of the sample with a 0.5% proportion. Moreover, the samples containing glass fibers exhibited lower shrinkage than the control samples. This can be illustrated by the HSC-Control, HSC-GF 0.5%, and 1%, aged for 7 days, with shrinkage values of 350 με, 187 με, and 151 με, respectively. The decreases in total shrinkage were 46.6% and 56.9%, respectively. According to a report by Zhang *et al.* (2020),[25] glass fibers reduced both total and free shrinkage of concrete by 7%, whereas polyester fibers achieved a reduction of 4% in both aspects. The report indicates that glass fibers are more effective in reducing total and free shrinkage due to having a higher modulus compared to polyester fibers.

Figure 8 shows that the sample with 0.5% polypropylene fibers exhibited less shrinkage than the control sample. Conversely, the proportion at 1% displayed greater shrinkage than that of the control sample. This is evident in the HSC-Control, HSC-PPF 0.5%, and 1%, aged for 7 days, which displayed shrinkage values of 350 με, 258 με, and 397 με, respectively. The total shrinkage decreased by 26.3% for PPF 0.5%, whereas it increased by 11.8% for PPF 1%. According to Saje *et al.* (2012),[12] previous research investigated the total shrinkage of concrete reinforced with polypropylene fibers.

The study found that fiber-reinforced composite materials

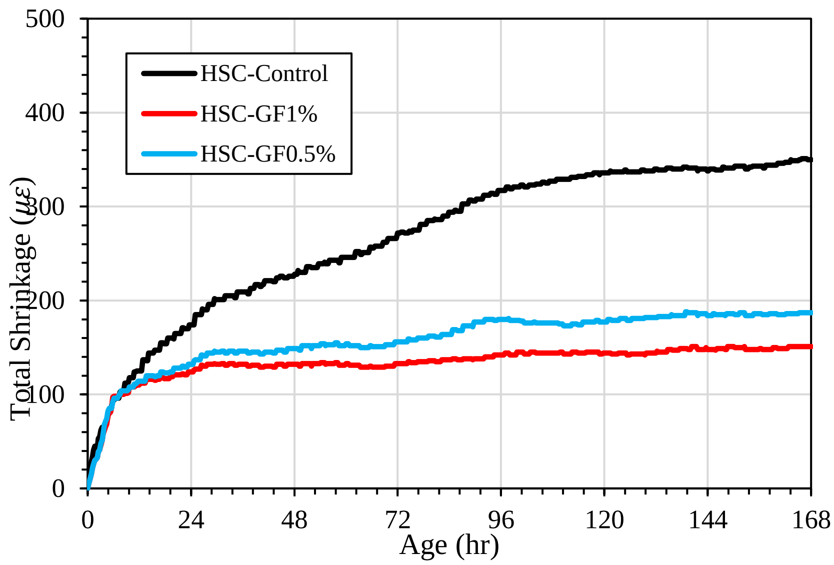

Fig. 7 Relationship between total shrinkage and age of HSC-control, HSC-GF0.5% and 1%.

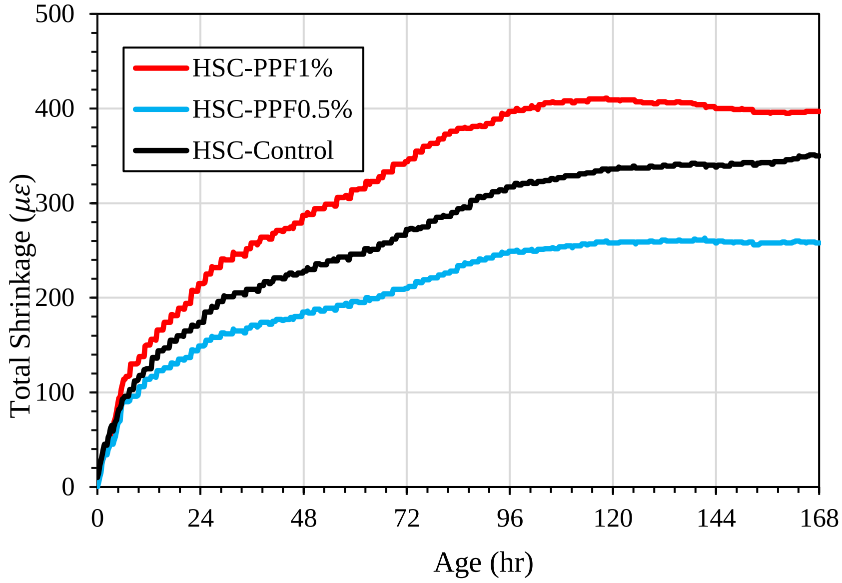

Fig. 8 Relationship between total shrinkage and age of HSC-control, HSC-PPF0.5% and 1%.

exhibited lower total shrinkage compared to concrete aggregates without fibers, showing reductions ranging from 17% to 29%.

The total shrinkage values of HSC-Control, HSC-GF, HSC-CF, and HSC-PPF at 0.5% were similar in the initial 24-hour period (Fig. 9). However, it became evident that the total shrinkage of the three fiber-added samples was lower compared to the control sample after 24 hours. These results underscore the efficacy of all three fiber types in reducing total shrinkage when appropriate proportions are added to high-strength concrete. GF fibers are recognized for their high tensile strength and modulus, whereas CF fibers serve as internal curing agents. Both CF and PPF fibers offer sufficient tensile strength. Collectively, these fiber characteristics play a crucial role in reducing total shrinkage in the cement matrix. Moreover, the test results reveal a direct relationship between total shrinkage and autogenous shrinkage. Samples with higher total shrinkage typically exhibit increased autogenous shrinkage. Understanding both internal temperature and total shrinkage is crucial for accurately assessing autogenous shrinkage.

3.5 Early-age autogenous shrinkage

The results of this autogenous shrinkage test consider the impact of the concrete internal temperature for a comprehensive analysis. As the heat generated during cement

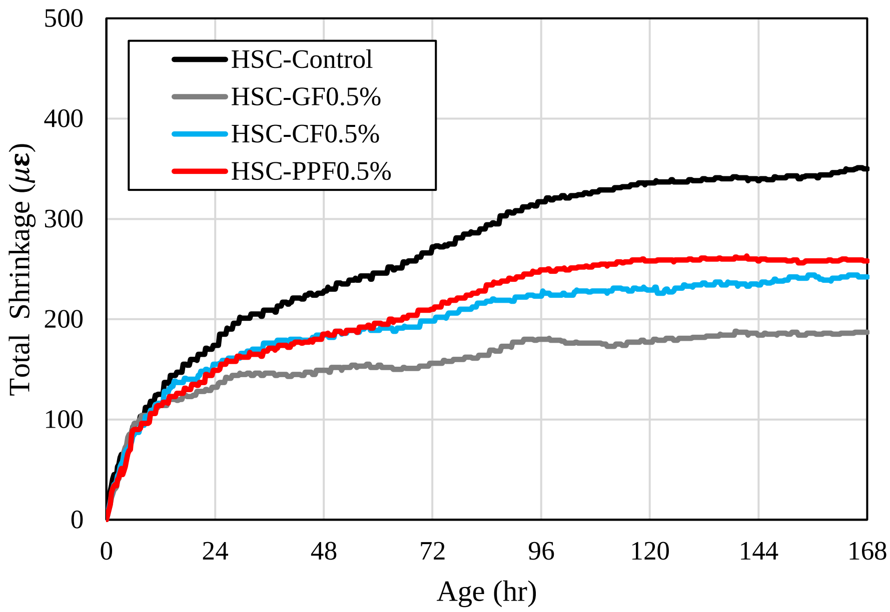

Fig. 9 Relationship between total shrinkage and age of HSC-control, HSC-GF0.5%, HSC-CF0.5% and HSC-PPF0.5%.

hydration can lead to fluctuations in the internal temperature, potentially affecting the expansion or contraction of the concrete, this is a critical consideration. After the concrete mixing process, the temperature initially increases above the ambient level and then gradually returns to its original state, as shown in Fig. 10. The rate of temperature change, whether an increase or decrease, varies depending on factors such as the concrete mix, test sample size, and environmental conditions. Consequently, the thermal element will always be integrated into total shrinkage, which can be expressed as follows[2-3]:

$$\varepsilon_{total}\,(t) = \varepsilon_{aut}\,(t) + \varepsilon_{thermal}(t) \quad (1)$$

$$\varepsilon_{thermal}\,(t) = \alpha(t)\; x\; [T(t) - T_0(t)] \quad (2)$$

$$\varepsilon_{aut}\,(t) = \varepsilon_{total}\,(t) - \alpha(t)\; x\; [T(t) - T_0(t)] \quad (3)$$

where $\varepsilon_{aut}\,(t)$ is the autogenous shrinkage (με), $\varepsilon_{total}\,(t)$ is the total shrinkage (με), $\alpha(t)$ is a coefficient of thermal expansion με/°C and can be taken as 10 με/°C,[2,3] $T(t)$ is the internal temperature (°C), and $T_0\,(t)$ is the ambient temperature (°C).

Figure 10 shows the relationship between the autogenous shrinkage and the age of the HSC-CF concrete. The autogenous shrinkage can be determined using Equation (3). A positive shrinkage value indicates that the concrete is contracting. The addition of 0.5% and 1% cellulose fibers effectively mitigates autogenous shrinkage. Interestingly, the concrete reinforced with 0.5% cellulose fiber and the control concrete had a similar tendency to shrink during the initial 24 hours. From this perspective, HSC-Control, HSC-CF 0.5%, and 1% aged for 7 days exhibited shrinkage values of 340 με, 241 με, and 205 με, respectively. The decreases in shrinkage were 29.1% and 39.7%, respectively. This decrease in shrinkage can be attributed to the presence of saturated cellulose fibers within the concrete. These fibers gradually release water, helping to maintain a balanced moisture level to offset moisture loss due to the cement hydration reaction. Thus, it appears that cellulose fibers are an internal curing material.[5] Additionally, cellulose fibers have the unique ability to bridge microcracks within the concrete matrix, thus contributing to the reduction in autogenous shrinkage. Therefore, even though the initial shrinkage was similar, using 1% cellulose fibers resulted in extra shrinkage reduction compared to 0.5% cellulose fibers.

Autogenous shrinkage can be determined using Equation (3). The inclusion of 0.5% and 1% glass fibers effectively inhibited the development of autogenous shrinkage in the concrete, as shown in Fig. 11. The control concrete exhibited more shrinkage than the HSC-GF 0.5% and 1% samples aged for 7 days, which exhibited shrinkage values of 340 με, 171 με, and 133 με, respectively. The decreases in shrinkage were 49.7% and 60.9%, respectively. These test results underscore the shrinkage-reducing effect of incorporating glass fibers into concrete. The decrease in autogenous shrinkage observed with the addition of glass fibers to high-strength concrete can be attributed to the non-shrinking nature of these fibers and their high elastic modulus in comparison to that of the matrix. Park *et al*. (2020) reported the significance of glass fibers, steel fibers, and carbon fibers possessing higher elastic moduli than normal synthetic fibers.[26] This higher modulus makes them effective at mitigating shrinkage within the cement matrix. When glass fibers are added and bonded to the matrix, they offer mechanical resistance to deformation, inhibiting the initiation, development, and propagation of microcracks in the

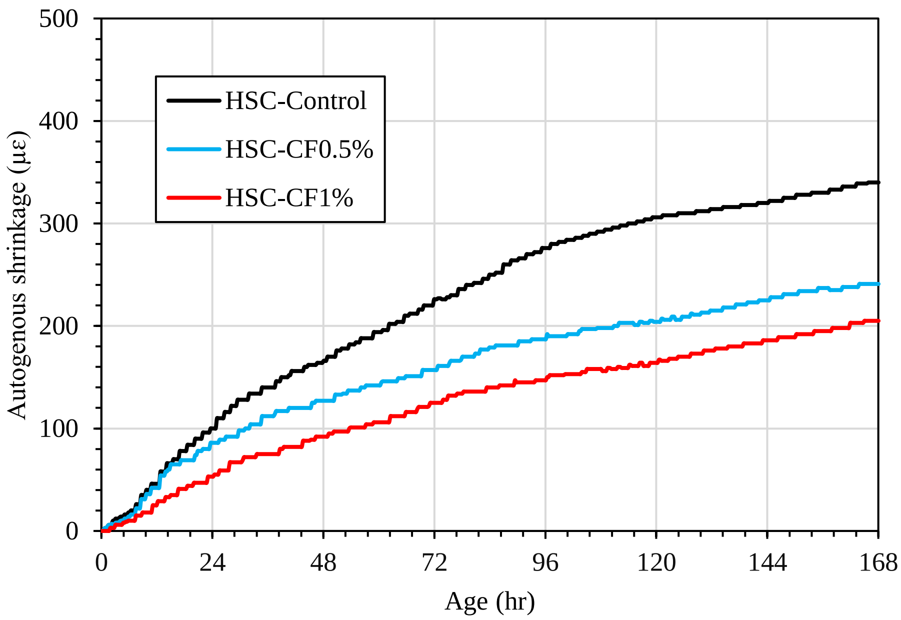

Fig. 10 Autogenous shrinkage of HSC-CF.

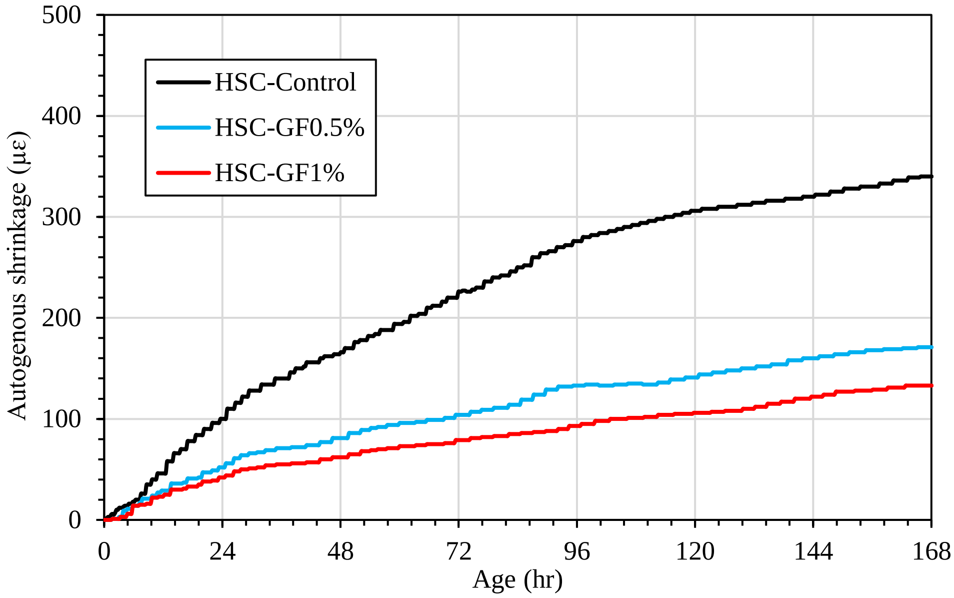

Fig. 11 Autogenous shrinkage of HSC-GF.

matrix. This results in a reduction in autogenous shrinkage in high-strength concrete. Additionally, Meng *et al*. (2018) reported that the autogenous shrinkage of high-performance concrete decreases with the incorporation of steel fibers and polyvinyl alcohol fibers.[27] This suggests that including fibers can effectively decrease autogenous shrinkage. These fibers may act as bridges, addressing small cracks and impeding crack propagation at an early stage.

Figure 12 shows the autogenous shrinkage of the HSC-PPF. Autogenous shrinkage can be determined using Equation (3). After the initial 24 hours, concrete with the addition of 0.5% fibers experiences less shrinkage than the control concrete. The HSC-Control and HSC-PPF 0.5% groups exhibited shrinkage at 7 days, with values of 340 με and 257 με, respectively. The decrease in shrinkage was 24.4%. This decrease in shrinkage highlights the influence of polypropylene fibers on the autogenous shrinkage of the concrete, which indicates the restraining ability of polypropylene fibers. The modulus of elasticity for fibers has a similar value as the modulus of elasticity for young concrete. Fibers have a positive influence on the distribution of stress and decrease the shrinkage strain.

In the case of 1% HSC-PPF, the shrinkage value at 7 days was 408 με. The increase in shrinkage was 16.7%. Compared to that of the control concrete, the shrinkage is greater due to the hindering effect of the polypropylene fibers. Autogenous contraction can only be restrained to a certain extent, and an excessively high proportion of fibers can lead to increased concrete shrinkage. Polypropylene fibers exhibit water absorption characteristics. In cases of excessive fiber content,

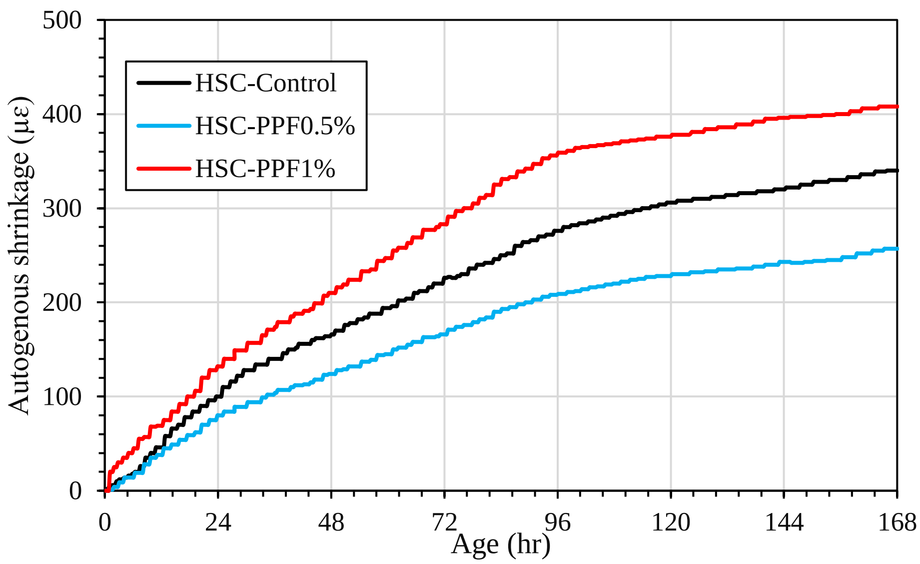

Fig. 12 Relationship between autogenous shrinkage and age of HSC-PPF.

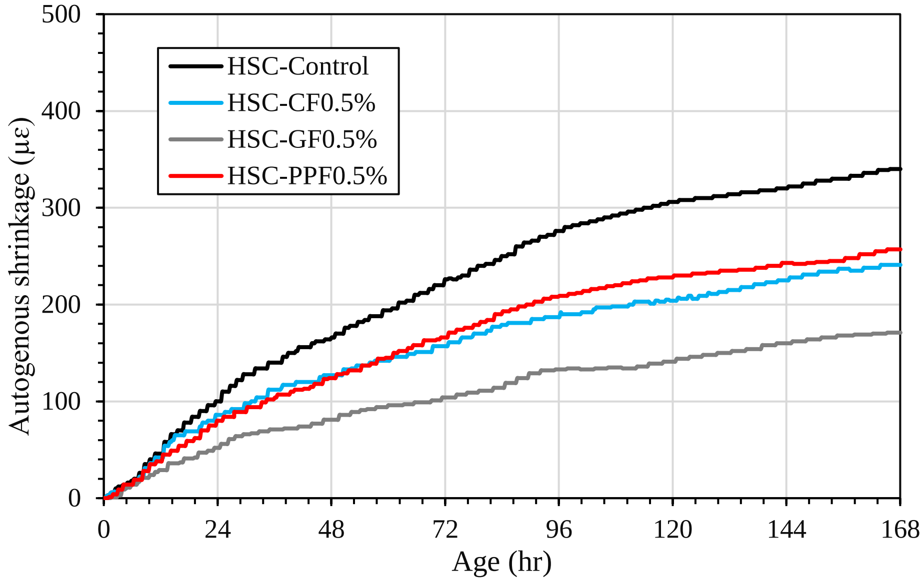

Fig. 13 Relationships between the autogenous shrinkage and age of the HSC-CF, HSC-GF, and HSC-PPF specimens.

these fibers absorb water, leading to a reduction in the water content of high-strength concrete and subsequent shrinkage. Research conducted by Shen *et al*. (2023) revealed that the PPF can hinder the development of early-age autogenous shrinkage in ultrahigh-performance concrete to a certain degree, and the effect of this obstacle decreases when increasing the volume proportion of the PPF.[28]

When comparing the autogenous shrinkage test results of high-strength concrete containing 0.5% CF, GF, and PPF fibers, as shown in Fig. 13, it was found that the HSC-GF had the lowest shrinkage. For HSC-CF and HSC-PPF, it was observed that, from the beginning up to 48 hours, the concrete samples containing polypropylene fibers exhibited less shrinkage than those containing cellulose fibers. However, the concrete samples containing cellulose fibers exhibited less shrinkage after 72 hours than those containing polypropylene fibers. It was also found that the shrinkage of both samples became similar. This phenomenon can be attributed to the polypropylene and cellulose fibers being weaker than glass fibers. Glass fibers possess high strength and are well dispersed in the cement matrix. Consequently, fiber forces may be transferred more effectively from the glass fibers, aiding in stress transfer and resulting in internal cracks that increase the resistance of the cement matrix.

3.6 Thermal behavior analysis

Figures 14-16 show the TGA/DTG results for CF, GF, and PPF added to HSC, respectively. The temperature vs. mass loss results varied greatly with the addition of each fiber. The evaluation was carried out at 600 degrees Celsius.

In the HSC-Control group, it is possible to identify two main peaks related to phase transformations from the DTG graphic shown in Figs. 14-16. The first peak before 160 °C is associated with the evaporation of free water and dehydration of ettringite in conjunction with gradual water loss from calcium silicate hydrates (CSH), with a residual weight of 97%. The second and smallest peak is at approximately 450 °C, and occurs with the dehydration of $Ca(OH)_2$; the mass loss is almost negligible.

Figure 14 shows the TGA/DTG test results for the HSC-CF1% and HSC-CF0.5% samples after the addition of each fiber. The first stage, with rapid moisture evaporation before 160°C, is similar to that of the HSC-Control but results in a lower residual weight of 93% and a higher weight loss rate of 0.8%. This can be attributed to the existence of additional water in the HSC-CF samples from the saturation of the fibers. The second and third phases encompass temperatures ranging from approximately 280-360 °C and 440-520 °C, with residual weights of 91% and 89%, respectively. The second phase mass loss refers to fiber decomposition, as CF possesses a melting temperature of approximately 270-300 °C, and the third phase is the dehydration of $Ca(OH)_2$. Notably, the addition of CF increased the amount of $Ca(OH)_2$ compared to that in the control sample. The internal curing property of CF gradually releases water and maintains the hydration of the cement, which produces $Ca(OH)_2$ that is not yet consumed in the interaction with SF. The pozzolanic reaction between SF particles and $Ca(OH)_2$ formed in the first stage of hydration consumes $Ca(OH)_2$ and produces additional CSH, resulting in compacted cement paste. The SF particles also contribute to densifying the microstructure by filling in gaps within the cement matrix and ITZ.[14] These results confirm that CF melts

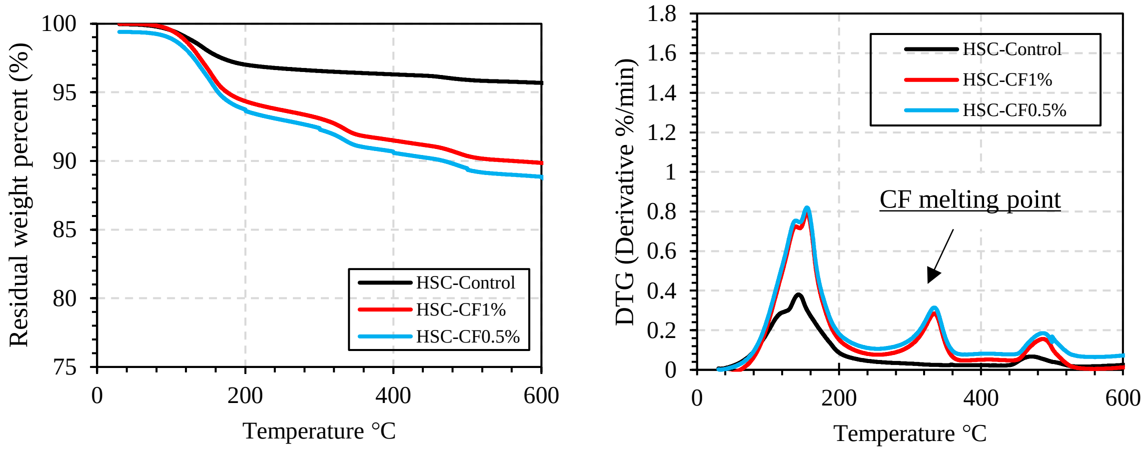

Fig. 14 TGA and DTG of HSC-CF.

at lower temperatures, which can decrease the internal water vapor pressure due to the generation of microcracks and prevent spalling at higher temperatures.

Figure 15 shows the TGA/DTG test results for the HSC-GF1% and HSC-GF0.5% samples. The thermal behavior encompasses two primary temperature ranges but is different from that of the CF addition profiles. The first period is characterized by an increase in mass loss occurring before 200 °C compared to that of the HSC-Control, resulting in a residual weight of 94% and a weight loss rate of 0.6%, associated with the free water and dehydration of cement hydration products. In the second period, a peak in DTG can be identified at approximately 450 °C from $Ca(OH)_2$ dehydration, resulting in a small weight loss and a weight loss of 93%. It is important to note that GF decomposition could not be identified, confirming that GF underwent significant decomposition after 900 °C. Consequently, GF cannot prevent spalling at temperatures below 600 °C.

The TGA/DTG results for the HSC-PPF1% and HSC-PPF0.5% samples are shown in Fig. 16. The thermal behavior can also be categorized into two primary temperature ranges. The first period, characterized by the highest peak in the DTG curve at temperatures between 40 °C and 200 °C, leads to a 93% residual weight. This phase exhibits a weight loss rate of 0.9% and corresponds to the cumulative loss of free water, decomposition of cement hydrates such as C-S-H, and mass loss from PPF decomposition, which results in a melting temperature of approximately 160-170°C. The second phase occurs at 450 °C and is caused by $Ca(OH)_2$ dehydration. The test results confirmed the low melting point of the PPF but decreased the pore pressure by enlarging the empty zone around the fibers and increasing the permeability at elevated temperatures, which is important for verifying the connectivity of channels to facilitate pore pressure release in dense HSC with PPF.[14]

As illustrated in Figs. 14-16, a comprehensive examination of the TGA/DTG test results enables a detailed analysis of weight changes during the heating process from lower to higher temperatures. It is evident that the addition of fibers influenced the thermal mass loss behavior in high-strength concrete. All three samples exhibited a distinct peak in the initial period, aligning with significant mass loss at

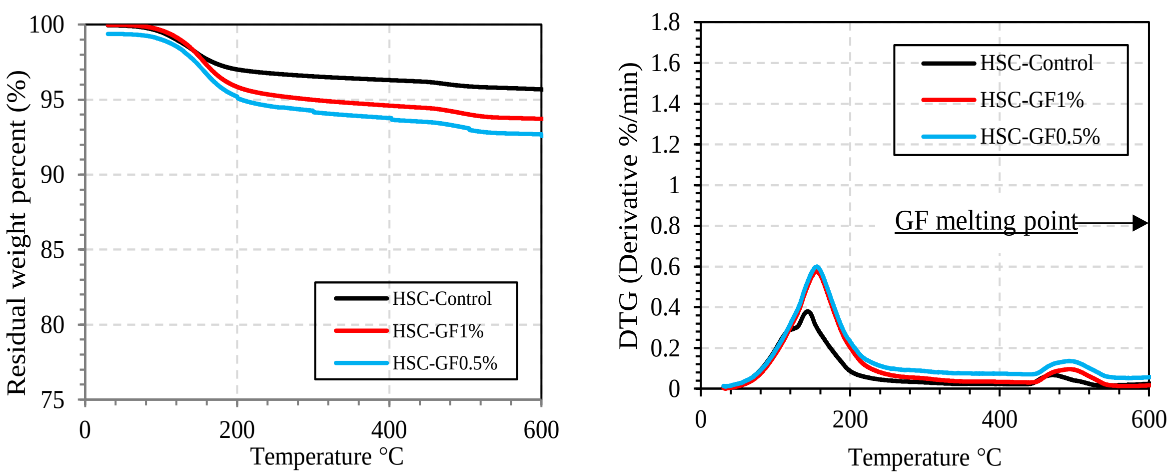

Fig. 15 TGA and DTG results for the HSC-GF.

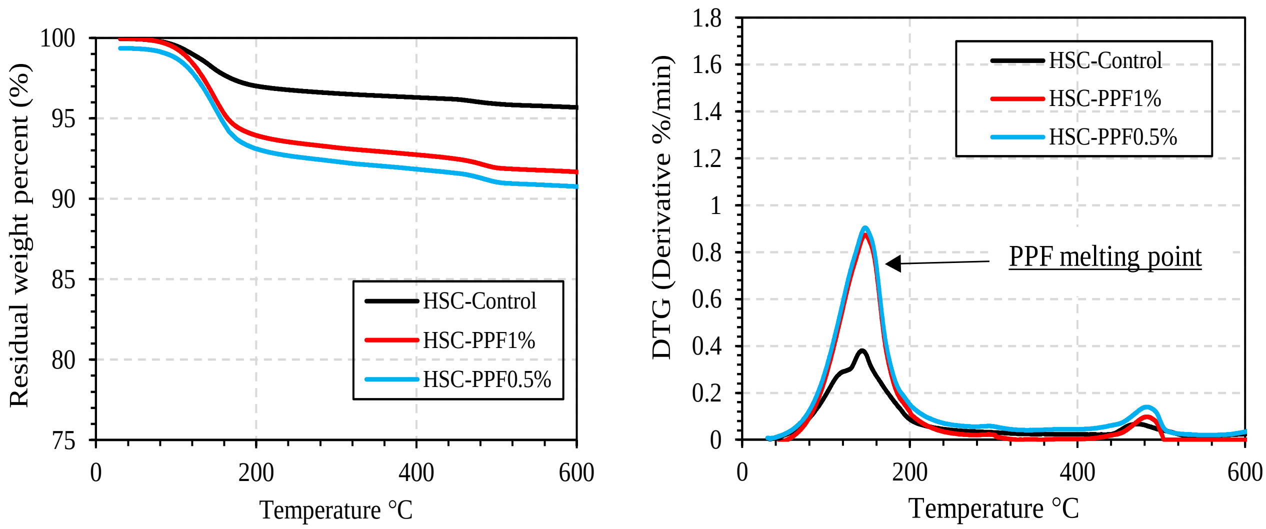

Fig. 16 TGA and DTG of HSC-PPF.

approximately 160 °C. Notably, concrete with fibers displayed a greater mass loss than did concrete without fibers at temperatures below 600 °C. The findings from the thermal analysis suggest that the presence of fibers may lower the internal pore pressure, indicating their applicability for use as an additive to prevent spalling at high temperatures.

4. Conclusions

Based on the results of experiments concerning the autogenous shrinkage and thermal behavior of high-strength concrete (HSC) reinforced with cellulose fibers (CF), glass fibers (GF), and polypropylene fibers (PPF) to mitigate autogenous shrinkage in the early stage of HSC, the incorporation of all three fiber types was proven to be effective in reducing shrinkage. However, achieving optimal shrinkage reduction requires the addition of fibers in appropriate proportions. GF exhibited the most substantial reduction in shrinkage at a 1% ratio, decreasing shrinkage by 69.9%, followed by CF, which aided in shrinkage reduction at a 1% ratio, decreasing shrinkage by 39.7%. PPF demonstrated effective shrinkage reduction at a 0.5% ratio, decreasing shrinkage by 24.4%. The internal temperature of the concrete in all samples did not exhibit significant differences. The thermal mass loss behavior of the fiber-reinforced HSC exhibited a peak at approximately 160 °C across all three samples. Below 600 °C, HSC with CF, GF, and PPF exhibited greater mass loss than did HSC-Control. These findings from the thermal behavior analysis suggest that the inclusion of fibers could decrease the internal pore pressure and could be used as an additive to mitigate spalling at elevated temperatures.

This study experimentally showed the positive effects of using CF, GF, and PPF in HSC at appropriate proportions to address autogenous shrinkage and spalling, which are two major concerns in HSC.

Acknowledgments

This research was funded by Thammasat School of Engineering (TSE), Thammasat University. Also, this research project was supported by the Thailand Science Research and Innovation Fundamental Fund fiscal year 2024, Thammasat University.

Conflict of Interest

There is no conflict of interest.

Supporting Information

Not applicable.

References

[1] D. Shen, X. Liu, Q. Li, L. Sun, W. Wang, Early-age behavior and cracking resistance of high-strength concrete reinforced with Dramix 3D steel fiber, *Construction and Building Materials*, 2019, **196**, 307-316, doi: 10.1016/j.conbuildmat.2018.10.125.

[2] D. Shen, C. Wen, P. Zhu, Y. Wu, Y. Wu, Influence of Barchip fiber on early-age autogenous shrinkage of high-strength concrete internally cured with super absorbent polymers, *Construction and Building Materials*, 2020, **264**, 119983, doi: 10.1016/j.conbuildmat.2020.119983.

[3] D.-Y. Yoo, J.-J. Park, S.-W. Kim, Y.-S. Yoon, Early age setting, shrinkage and tensile characteristics of ultra high-performance fiber reinforced concrete, *Construction and Building Materials*, 2013, **41**, 427-438, doi: 10.1016/j.conbuildmat.2012.12.015.

[4] L. Wu, N. Farzadnia, C. Shi, Z. Zhang, H. Wang, Autogenous shrinkage of high-performance concrete: a review, *Construction and Building Materials*, 2017, **149**, 62-75, doi: 10.1016/j.conbuildmat.2017.05.064.

[5] S. Kawashima, S. P. Shah, Early-age autogenous and drying

shrinkage behavior of cellulose fiber-reinforced cementitious materials, *Cement and Concrete Composites*, 2011, **33**, 201-208, doi: 10.1016/j.cemconcomp.2010.10.018.
[6] J. Liu, C. Lv, Research progress on durability of cellulose fiber-reinforced cement-based composites, *International Journal of Polymer Science*, 2021, **2021**, 1014531, doi: 10.1155/2021/1014531.
[7] A. Guo, Z. Sun, J. Satyavolu, Impact of modified kenaf fibers on shrinkage and cracking of cement pastes, *Construction and Building Materials*, 2020, **264**, 120230, doi: 10.1016/j.conbuildmat.2020.120230.
[8] Y. C. Choi, Hydration and internal curing properties of plant-based natural fiber-reinforced cement composites, *Case Studies in Construction Materials*, 2022, **17**, e01690, doi: 10.1016/j.cscm.2022.e01690.
[9] G. W. Lee, Y. C. Choi, Effect of abaca natural fiber on the setting behavior and autogenous shrinkage of cement composite, *Journal of Building Engineering*, 2022, **56**, 104719, doi: 10.1016/j.jobe.2022.104719.
[10] J. H. Ideker, J. Bañuelos, The use of synthetic blended fibers to reduce cracking risk in high-performance concrete, 2014.
[11] M. Serdar, A. Baričević, M. Jelčić Rukavina, M. Pezer, D. Bjegović, N. Štirmer, Shrinkage behaviour of fibre reinforced concrete with recycled tyre polymer fibres, *International Journal of Polymer Science*, 2015, **2015**, 145918, doi: 10.1155/2015/145918.
[12] D. Saje, B. Bandelj, J. Šušteršic, J. Lopatic, F. Saje, Autogenous and drying shrinkage of fibre reinforced high-performance concrete, *Journal of Advanced Concrete Technology*, 2012, **10**, 59-73, doi: 10.3151/jact.10.59.
[13] F. Ullah, F. Al-Neshawy, J. Punkki, Early age autogenous shrinkage of fibre reinforced concrete, *Nordic Concrete Research*, 2018, **59**, 59-72, doi: 10.2478/ncr-2018-0015.
[14] M. Amran, S.-S. Huang, A. M. Onaizi, G. Murali, H. S. Abdelgader, Fire spalling behavior of high-strength concrete: a critical review, *Construction and Building Materials*, 2022, **341**, 127902, doi: 10.1016/j.conbuildmat.2022.127902.
[15] P. Kalifa, G. Chene, C. Galle, High-temperature behavior of HPC with polypropylene fibers: From spalling to microstructure, *Cement and Concrete Research*, 2001, **31**, 1487-1499, doi: 10.1016/S0008-8846(01)00596-8.
[16] T. Lee, G. Kim, G. Choe, E. Hwang, J. Lee, D. Ryu, J. Nam, Spalling resistance of fiber-reinforced ultra-high-strength concrete subjected to the ISO-834 standard fire curve: effects of thermal strain and water vapor pressure, *Materials*, 2020, **13**, 3792, doi: 10.3390/ma13173792.
[17] V. K. R. Kodur, M. A. Sultan, Effect of temperature on thermal properties of high-strength concrete, *Journal of Materials in Civil Engineering*, 2003, **15**, 101-107, doi: 10.1061/(asce)0899-1561(2003)15: 2(101).
[18] American society for testing materials. Committee C-1 on cement, Standard Performance specification for hydraulic cement. ASTM International, 2003.
[19] American Society for Testing and Materials. Committee C-09 on Concrete and Concrete Aggregates, Standard Specification for Chemical Admixtures for Concrete, ASTM International, 2017.
[20] American Society for Testing and Materials, ASTM C 618-Standard specification for coal fly ash and raw or calcined natural pozzolan for use in concrete, West Conshohocken: ASTM, 2012.
[21] ACI Committee, Guide for selecting proportions for high strength concrete using Portland cement and other cementitious materials, American Concrete Institute, 2008.
[22] M. N. Amin, J.-S. Kim, T. T. Dat, J.-K. Kim, Improving test methods to measure early age autogenous shrinkage in concrete based on air cooling, *The IES Journal Part A: Civil & Structural Engineering*, 2010, **3**, 244-256, doi: 10.1080/19373260.2010.522314.
[23] J. Liu, K. Yan, X. Zhao, Y. Hu, Prediction of autogenous shrinkage of concretes by support vector machine, *International Journal of Pavement Research and Technology*, 2016, **9**, 169-177, doi: 10.1016/j.ijprt.2016.06.003.
[24] M. Kurpińska, M. Pawelska-Mazur, Y. Gu, F. Kurpiński, The impact of natural fibers' characteristics on mechanical properties of the cement composites, *Scientific Reports*, 2022, **12**, 20565, doi: 10.1038/s41598-022-25085-6.
[25] J. Zhang, V. C. Li, Influences of fibers on drying shrinkage of fiber-reinforced cementitious composite, *Journal of Engineering Mechanics*, 2001, **127**, 37-44, doi: 10.1061/(asce)0733-9399(2001)127: 1(37).
[26] J.-J. Park, S. Kim, W. Shin, H.-J. Choi, G.-J. Park, D.-Y. Yoo, High-performance photocatalytic cementitious materials containing synthetic fibers and shrinkage-reducing admixture, *Materials*, 2020, **13**, 1828, doi: 10.3390/ma13081828.
[27] W. Meng, K. H. Khayat, Effect of hybrid fibers on fresh properties, mechanical properties, and autogenous shrinkage of cost-effective UHPC, *Journal of Materials in Civil Engineering*, 2018, **30**, 04018030, doi: 10.1061/(asce)mt.1943-5533.0002212.
[28] D. Shen, C. Liu, Y. Luo, H. Shao, X. Zhou, S. Bai, Early-age autogenous shrinkage, tensile creep, and restrained cracking behavior of ultra-high-performance concrete incorporating polypropylene fibers, *Cement and Concrete Composites*, 2023, **138**, 104948, doi: 10.1016/j.cemconcomp.2023.104948.

